Published by Institute of Physics Publishing for SISSA

Received: *February 17, 2006*
Accepted: *March 27, 2006*
Published: *April 24, 2006*

Excursions beyond the horizon: black hole singularities in Yang-Mills theories (I)

Guido Festuccia and Hong Liu

Center for Theoretical Physics, Massachusetts Institute of Technology
Cambridge, Massachusetts, 02139, U.S.A.
E-mail: guido@mit.edu, hong_liu@lns.mit.edu

Abstract: We study black hole singularities in the AdS/CFT correspondence. These singularities show up in CFT in the behavior of finite-temperature correlation functions. We first establish a direct relation between space-like geodesics in the bulk and momentum space Wightman functions of CFT operators of large dimensions. This allows us to probe the regions inside the horizon and near the singularity using the CFT. Information about the black hole singularity is encoded in the exponential falloff of finite-temperature correlators at large imaginary frequency. We construct new gauge invariant observables whose divergences reflect the presence of the singularity. We also find a UV/UV connection that governs physics inside the horizon. Additionally, we comment on the possible resolution of the singularity.

Keywords: AdS-CFT Correspondence, Black Holes in String Theory.

JHEP04(2006)044

Contents

JHEP04(2006)044

1. Introduction

The AdS/CFT correspondence [1 – 3] provides exciting avenues for exploring various issues in quantum gravity. An important question that the AdS/CFT correspondence may shed light on is that of the nature of spacelike singularities, like the Big Bang or the singularity of a Schwarzschild black hole. A good laboratory for studying spacelike singularities is an eternal black hole in anti-de Sitter (AdS) spacetime. It has been conjectured that quantum gravity in an AdS_{d+1} black hole background is described by a boundary conformal field theory on $S^{d-1} \times \mathbb{R}$ at a temperature given by the Hawking temperature of the black hole [2, 4, 5].[1]

[1] More precisely, an AdS black hole appears as a saddle point in the path integral of boundary theories in the large N limit.

The conventional wisdom regarding singularities is that they signal the breakdown of classical gravity and should go away when stringy or quantum gravitational effects are taken into account. Since in AdS/CFT, classical gravity corresponds to the large N and large 't Hooft coupling limit of the boundary theory,[2] one expects that finite N or finite 't Hooft coupling effects may resolve these singularities [6, 5]. Such considerations suggest the following strategy:

1. Identify manifestations of the black hole singularity in the large N and large 't Hooft coupling limit of the finite temperature boundary theory;

2. From these manifestations, understand the precise physical mechanism through which the finite N or finite 't Hooft coupling effects may resolve the singularity.

In the boundary theory, the physical observables are correlation functions of gauge invariant operators. This means that the physics of singularities should be encoded in the behavior of boundary correlation functions in appropriate limits.

One of the obstacles[3] in understanding black hole singularities from finite temperature boundary theory is that the singularities are hidden behind event horizons. The boundary conformal field theory evolves through the bulk Schwarzschild time, i.e. from the point of view of an external observer, and does not appear to directly describe the physics beyond the horizon. In other words, if time evolution inside the horizon of a black hole is to be described by the boundary theory, time has to be *holographically* generated. This makes the problem particularly challenging, while at the same time exciting. In particular, understanding physics beyond the horizon should shed light on how to holographically describe a Big Bang cosmological spacetime.[4]

A number of authors [5, 7 – 17] have explored how to extract physics beyond the horizon from the boundary theory correlation functions.[5] In particular, Fidkowski et al [12] found an interesting but subtle signal of the singularity in the boundary correlators. They found that AdS_{d+1} black holes with dimension $d \geq 3$ contain spacelike geodesics, connecting two asymptotic boundaries, which could get arbitrarily close to the singularity. The authors further argued that such geodesics imply the presence of poles on secondary sheets of the analytically continued coordinate space correlation functions in the large operator dimension limit.

Here we further explore the manifestations of the black hole singularity in the boundary theory and discuss their implications for the resolution of the singularity.

We will establish a direct relation between space-like geodesics in the bulk spacetime and the large operator dimension limit of momentum space Wightman functions in the boundary theory. We show that physics in the region beyond the horizon is encoded

[2] While we are interested in black holes in all dimensions, when talking about boundary theories, we will more specifically have in mind $d = 4$, which are $SU(N)$ Yang-Mills theories.

[3] in addition to the standard difficulties to decode the local bulk physics from boundary theories

[4] The regions around the past and future singularities of a black hole can also be viewed as Big Bang or Big Crunch cosmologies.

[5] See also [18, 19]. For other recent discussion of spacelike singularities in AdS/CFT, see e.g. [20 – 22].

JHEP04(2006)044

in the behaviors of boundary correlation functions along the imaginary frequency axis. In particular, this gives a clear indication that the "time" inside the horizon is holographically generated from the boundary theory. The presence of the curvature singularity leads to certain exponential falloff of the correlation functions near the imaginary infinity. We also construct new gauge invariant observables which have singularities precisely reflecting the curvature singularity of the black hole.

In this paper we will present the main idea using the example of an AdS_5 Schwarzschild black hole, leaving technical details and more extensive discussions of other examples to a longer companion paper [23]. In [24] we develop a new method for computing the large mass quasi-normal frequencies of the black hole, whose knowledge is crucial for the discussion of this paper and [23].

The plan of the paper is as follows. In section 2, we review the relevant black hole geometry and the computation of boundary Wightman function in AdS/CFT. In section 3, we establish a connection between bulk spacelike geodesics and boundary Wightman functions in the large operator dimension limit. In section 4, we study the manifestation of the singularities in Yang-Mills theory. We conclude in section 5 with a discussion of the possible resolution of singularities at finite N.

2. Boundary correlation functions from AdS/CFT

2.1 Black hole geometry

We will consider big black holes in AdS_5, which have a positive specific heat and are the dominant contribution to the thermal canonical ensemble of the boundary Yang-Mills theory when the temperature is sufficiently high [25].

The metric for a Schwarzschild black hole in an AdS_5 spacetime is given by

$$ds^2 = -f(r)dt^2 + f(r)^{-1}dr^2 + r^2 d\Omega_3^2 \tag{2.1}$$

with

$$\begin{aligned} f(r) &= r^2 + 1 - \frac{\mu}{r^2} = \frac{1}{r^2}(r^2 - r_0^2)(r^2 + r_1^2), \\ r_1^2 &= 1 + r_0^2, \qquad \mu = r_0^2 r_1^2 \end{aligned} \tag{2.2}$$

where μ is proportional to the mass of the black hole and the event horizon is at $r = r_0$. r_0, r_1 can be solved in terms of μ. We have set the curvature radius of AdS to be unity, as we will do throughout the paper. As $r \to \infty$, the metric goes over to that of global AdS with t identified as the boundary time. The fully extended black hole spacetime has two disconnected time-like boundaries, each of topology $S^3 \times \mathbb{R}$.

It is often convenient to use the tortoise coordinate

$$z = \int_r^\infty \frac{dr}{f(r)} = -\frac{\beta}{4\pi} \log\left(\frac{r - r_0}{r + r_0}\right) + \frac{\widetilde{\beta}}{2\pi} \tan^{-1} \frac{r_1}{r} \tag{2.3}$$

with

$$\beta = \frac{2\pi r_0}{r_0^2 + r_1^2}, \qquad \widetilde{\beta} = \frac{2\pi r_1}{r_0^2 + r_1^2} \ . \tag{2.4}$$

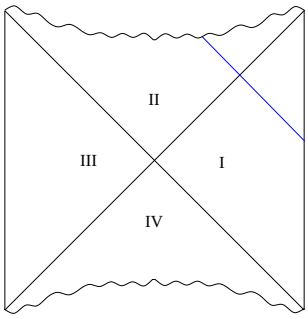

Figure 1: Penrose diagram for the AdS black hole. There are two asymptotic AdS regions, which are space-separated from each other. A null geodesic going from the boundary to the singularity is indicated in the figure.

The region outside the horizon corresponds to $z \in (0, +\infty)$ with $z = 0$ at the boundary and $z \to +\infty$ at the horizon. β is the inverse Hawking temperature. To have a feeling of the physical meaning of $\widetilde{\beta}$ we note that the *complex Schwarzschild time* that it takes for a radial null geodesic to go from the boundary to the singularity is given by

$$\pm \int_0^\infty \frac{dr}{f(r)} = \pm \frac{1}{4}(\widetilde{\beta} \pm i\beta) \tag{2.5}$$

where the imaginary part of the integral arises by going around the pole at $r = r_0$ in the complex r-plane. A nonzero $\widetilde{\beta}$ implies that the Penrose diagram for the black hole is not a square, as was first pointed out in [12]. It is convenient to introduce a complex quantity

$$\mathcal{B} = \widetilde{\beta} + i\beta = \frac{2\pi(r_1 + ir_0)}{r_0^2 + r_1^2} = \frac{2\pi}{r_1 - ir_0} \tag{2.6}$$

which will be important in our discussion. One can invert (2.3) to find $r(z)$. In particular, for $\mathrm{Re} z > \frac{\widetilde{\beta}}{4}$, r is a one-to-one periodic function of z with period $i\frac{\beta}{2}$.

We will consider the complexified Kruskal spacetime in which points related by

$$t \to t + i\frac{m+n}{2}\beta, \qquad z \to z + i\frac{m-n}{2}\beta, \quad m, n \in \mathbf{Z} \tag{2.7}$$

are identified. The Lorentzian section 1 of the complexified spacetime can be conveniently described using (t, z) with constant imaginary parts. For example, up to identifications (2.7), region III can be specified by

$$\mathrm{Im}\, t = -\frac{i\beta}{2}, \qquad \mathrm{Im}\, z = 0\,. \tag{2.8}$$

2.2 Boundary Wightman functions

Now consider an operator $\mathcal{O}$ in the boundary theory corresponding to a bulk field ϕ of mass m. In the supergravity limit, the conformal dimension of $\mathcal{O}$ is given by [3, 2]

$$\Delta = \frac{d}{2} + \nu, \qquad \nu = \sqrt{\frac{d^2}{4} + m^2}\,. \tag{2.9}$$

Thermal boundary two-point functions of $\mathcal{O}$ can be obtained from free bulk Green functions of ϕ in the Hartle-Hawking vacuum by taking the arguments of ϕ to the boundary (see e.g. [26, 27]).[6] For example, the boundary Wightman function is obtained by

$$G_+(x,x') = \lim_{r,r'\to\infty} (2\nu r^\Delta)(2\nu r'^\Delta)\mathcal{G}_+(x,r;x',r') \tag{2.10}$$

where $\mathcal{G}_+$ and G_+ denote the bulk and boundary correlation functions respectively

$$G_+(x,x') = \mathrm{Tr}\left[e^{-\beta H}\mathcal{O}(x)\mathcal{O}(x')\right], \tag{2.11}$$

$$\mathcal{G}_+(x,r;x',r') = \left\langle 0|\phi(r,x)\phi(r',x')|0\right\rangle_{HH} . \tag{2.12}$$

In the above equations we used the notation $x = (t,e)$ with e denoting a point on S^3 and the subscript "HH" denotes the Hartle-Hawking vacuum. Going to momentum space (2.10) becomes (see the appendix for a definition of the Fourier transform)

$$G_+(\omega,l) = \lim_{r,r'\to\infty} (2\nu r^\Delta)(2\nu r'^\Delta)\mathcal{G}_+(\omega,l;r,r') , \tag{2.13}$$

where l denotes the angular momentum on S^3. The Feynmann (retarded) propagator in the bulk leads to the Feynmann (retarded) Green function on the boundary by the same procedure. In this paper we will focus on G_+ for reasons to be commented on later.

Since the extended black hole background has two asymptotic boundaries, we can also take r and r' to different boundaries. Such points are always space-like separated in the bulk and lead to boundary correlation functions of complex time separation (see equation (2.8))

$$G_{12}(t) = \mathrm{Tr}\left[e^{-\beta H}\mathcal{O}(t-i\beta/2)\mathcal{O}(0)\right] = G_+(t-i\beta/2) \tag{2.14}$$

where we have suppressed the boundary spatial coordinates for notational simplicity. $G_+(t)$ is analytic for $-\beta < \mathrm{Im}t < 0$ and the two-sided correlator $G_{12}(t)$ can be obtained from $G_+(t)$ by simple analytic continuation.[7]

$\mathcal{G}_+$ can be found in terms of solutions to the Laplace equation for ϕ following the standard free field quantization procedure. Let

$$\phi = e^{-i\omega t}Y_I(e)r^{-\frac{d-1}{2}}\psi(\omega,p;r),$$

with $Y_I(e)$ denoting scalar spherical harmonics on S^3 (see the appendix for notations on spherical harmonics). The Laplace equation for ϕ can then be written in terms of the tortoise coordinate as a Schrodinger equation for ψ

$$\left(-\partial_z^2 + V_l(z) - \omega^2\right)\psi = 0 . \tag{2.15}$$

[6] For discussion of boundary Lorentzian correlation functions in the supergravity approximation, see also [28 – 31].

[7] In contrast, the Feynman and retarded functions have singularities in the range $-\frac{\beta}{2} < \mathrm{Im}t < 0$.

$V_l(z)$ can be expressed through $r(z)$ as

$$V_l(z) = f(r)\left[\frac{(l+1)^2-\frac{1}{4}}{r^2}+\nu^2-\frac{1}{4}+\frac{9\mu}{4r^4}\right]. \tag{2.16}$$

For real $l > 0$, $V_l(z)$ is a monotonically decreasing function of $z \in (0,\infty)$. Near the boundary,

$$V_l \approx \frac{\nu^2-\frac{1}{4}}{z^2}, \qquad z \to 0\ , \tag{2.17}$$

and near the horizon

$$V_l \propto e^{-\frac{4\pi}{\beta}z} \to 0, \qquad z \to +\infty\ . \tag{2.18}$$

For any given real ω the Schrodinger equation (2.15) has a unique normalizable mode $\psi_{\omega l}$, which we will take to be real. We normalize it at the horizon as (δ_ω is a phase shift)

$$\psi_{\omega l}(z) \approx e^{-i\omega z - i\delta_\omega} + e^{i\omega z + i\delta_\omega}, \qquad z \to +\infty\ . \tag{2.19}$$

As $z \to 0$, $\psi_{\omega l}$ has the form

$$\psi_{\omega l} \approx C(\omega,l) z^{\frac{1}{2}+\nu} + \cdots, \qquad z \to 0 \tag{2.20}$$

where the constant C is fixed by the normalization of (2.19). It is easy to check that $\psi_{\omega l}$ is even in ω.

Using the mode expansion of ϕ in the Hartle-Hawking vacuum, the bulk Wightman propagator $\mathcal{G}_+$ (2.14) in momentum space can be written in terms of $\psi_{\omega l}$ as

$$\mathcal{G}_+(\omega,l;r,r') = \frac{1}{2\omega}\frac{e^{\beta\omega}}{e^{\beta\omega}-1}(rr')^{-\frac{d-1}{2}}\psi_{\omega l}(r)\psi_{\omega l}(r') \tag{2.21}$$

which leads to the boundary G_+ upon using (2.13) and (2.20)

$$G_+(\omega,l) = \frac{(2\nu)^2}{2\omega}\frac{e^{\beta\omega}}{e^{\beta\omega}-1}C^2(\omega,l) \tag{2.22}$$

G_+ is to be evaluated for real ω, l and can be analytically continued to general complex ω and l.

2.3 Analytic properties

Equations (2.21) and (2.22) indicate that the boundary Yang-Mills theory has a *continuous* spectrum in the large N and large 't Hooft coupling limit, despite being on a compact space. At finite N, the theory should have a discrete spectrum on S^3. In the bulk the continuous spectrum arises due to the presence of the horizon.

The analytic properties of G_+ in the complex ω-plane for a given l can be deduced by applying standard techniques of scattering theory to (2.15). The fact that r is a periodic function of the tortoise coordinate with a period $i\frac{\beta}{2}$ implies that: [23]

1. The poles in the prefactor $\frac{1}{\omega(e^{\beta\omega}-1)}$ cancel with zeros of C^2. G_+ is analytic at $\omega = 0$ and $\omega = \frac{2\pi i n}{\beta}$, $n \in \mathbf{Z}$.

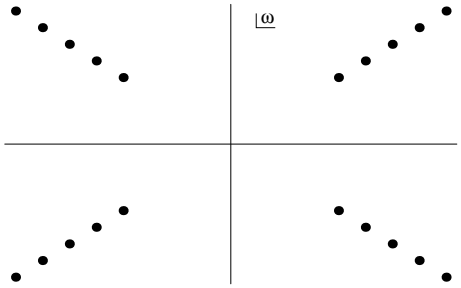

Figure 2: Poles for $G_+(\omega, l)$ for $l = 0$ in the complex ω-plane. We use $r_0 = 1, r_1 = \sqrt{2}$.

2. The only singularities of G_+ in the complex ω-plane are poles. The locations of the poles obey a reflection symmetry: if there is a pole at ω_0, then there are poles at $-\omega_0, \omega_0^*, -\omega_0^*$.

These two features are quite generic, applicable to AdS black holes of all dimensions. The poles of G_+ in the lower half ω-plane coincide with those of the retarded propagator G_R and correspond to quasi-normal frequencies of the black hole background. Since it is not known how to solve the Schrodinger equation (2.15) exactly, the determination of the quasi-normal poles is a difficult mathematical problem.

When $l = 0$ (or small compared to ν or ω), the problem simplifies and various methods [32 – 36] can be used to determine the locations of poles of G_+ approximately. One finds that there are four infinite lines of poles as indicated in figure 2. The poles in the upper right quadrant are given by [24]

$$\omega \approx \frac{2\pi}{\overline{\mathcal{B}}}\nu + \omega_0 + \frac{4\pi n}{\overline{\mathcal{B}}}, \qquad n = 0, 1, \cdots \tag{2.23}$$

The other lines are obtained by reflections. ω_0 in (2.23) is a constant of $O(1)$ (independent of ν) whose exact value is not relevant here.[8]

The quasi-normal frequencies for $l \neq 0$ and other dimensions are more complicated to find and will be discussed in [24].

3. Boundary Wightman functions and bulk geodesics

3.1 A semi-classical approximation

We now develop a "semi-classical" approximation to equation (2.15), in the following large ν limit

$$\omega = \nu u, \qquad l + 1 = \nu k, \qquad \nu \gg 1 \ , \tag{3.1}$$

i.e. we take the mass m of ϕ to be large and "measure" the frequency ω and angular momentum l in units of m. With $\psi = e^{\nu S}$ equation (2.15) becomes

$$-(\partial_z S)^2 - \frac{1}{\nu}\partial_z^2 S + V(z) + \frac{1}{\nu^2}Q(z) = u^2 \tag{3.2}$$

[8]The accuracy of equation (2.23) increases with n. A comparison with the numerical results obtained in [32] shows that it appears to work well even for n small.

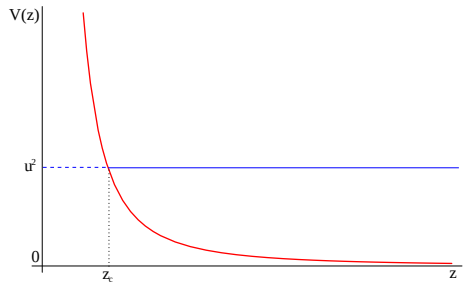

Figure 3: The potential $V(z)$ with $\mu = 10$ and $k = 0$ is shown. z_c is the turning point. Dashed and solid lines indicate the classically forbidden and allowed regions respectively.

with

$$V(z) = f(r)\left(1 + \frac{k^2}{r^2}\right), \qquad Q(z) = f(r)\left[-\frac{1}{4r^2} - \frac{1}{4} + \frac{9\mu}{4r^4}\right] . \tag{3.3}$$

With $k^2 \geq 0$ the leading order potential $V(z)$ is a monotonically decreasing function for $z \in (0, +\infty)$ as indicated in figure 3. For scattering sates with $u > 0$, (3.2) can be solved order by order in $1/\nu$ expansion using the standard WKB method. In the classically forbidden region (see figure 3), the exponentially decreasing solution can be written as

$$\psi_{\omega l}^{(wkb)}(r) = \frac{1}{\sqrt{f\kappa_r}} e^{\nu \mathcal{Z}} \left(1 + O\left(\nu^{-1}\right)\right) \tag{3.4}$$

with[9]

$$\mathcal{Z}(r) = -\int_{r_c}^{r} dr'\, \kappa_r(r'), \qquad \kappa_r = \frac{1}{f}\sqrt{V(r) - u^2} . \tag{3.5}$$

r_c in the lower integration limit of (3.5) is the turning point, given by the real positive root of the equation

$$V(r) = f(r)\left(1 + \frac{k^2}{r^2}\right) = u^2 . \tag{3.6}$$

For $u^2 > 0$, equation (3.6) has a unique positive root $r_c > r_0$. $\mathcal{Z}$ satisfies the equation

$$f\mathcal{Z}'^2 - \frac{k^2}{r^2} + \frac{1}{f}u^2 = 1 \tag{3.7}$$

with $\mathcal{Z}'(r_c) = 0$. Note that we have written the above equations in terms of r for convenience. One can equivalently write them in terms of the tortoise coordinate z. The expressions in terms of r are more convenient to visualize the analytic continuation to be discussed later.

The expression for $\psi_{\omega l}^{(wkb)}$ in the classically allowed region of the potential (3.3) (i.e. for $z_c < z$ or $r_0 < r < r_c$) follows from the standard connection formula, from which one can determine the relative normalization between $\psi_{\omega l}^{(wkb)}$ of (3.4) and $\psi_{\omega l}$ of (2.19) to be

$$\psi_{\omega l}^{(wkb)} = \frac{1}{\sqrt{u}}\psi_{\omega l}, \qquad u > 0, \quad \nu \to \infty \tag{3.8}$$

[9]The branch cuts for κ_r on the complex r-plane are chosen so that they do not intersect the integration contour in $\mathcal{Z}$.

From (3.8) we find that in the limit (3.1) the boundary Wightman function G_+ can be expanded as

$$G_+(\omega, l) \approx 2\nu\, e^{\nu Z(u,k)} \left(1 + O(\nu^{-1})\right) + \text{subdominant terms}, \qquad \omega > 0 \tag{3.9}$$

with

$$Z(u,k) = 2 \lim_{r\to\infty} \left(\log r - \int_{r_c}^{r} dr'\, \kappa_r(r') \right) . \tag{3.10}$$

Higher order $1/\nu$ corrections in (3.9) can also be obtained from (3.2) using the standard WKB procedure. In particular, the term proportional to $Q(z)$ will be important at order ν^{-1}. There could also be subdominant terms in (3.9) coming from reflections at other (complex) turning points of $V(r)$.

While equations (3.9)–(3.10) were obtained for $u > 0$ and $k \geq 0$, they can be analytically continued to the full complex u and k-planes. We will show in section 4 that the analytic continuation allows us to probe the region beyond the horizon.

3.2 Relation with geodesics

We expect $Z(u,k)$ in (3.10) to have a simple interpretation in terms of bulk geodesics. The reason is that in the large mass limit, the propagation of bulk field ϕ should approximately follow geodesic paths. Thus we expect a direct relation between the WKB approximation of the last subsection with the geodesic approximation. The scaling in (3.1) simply defines u as the "velocity" in t direction and k as the "angular velocity" on S^3.

Due to translational invariance in t and isometries on S^3, a bulk spacelike geodesic is characterized by the integrals of motion

$$E = f\frac{dt}{ds}, \qquad q = r^2 \frac{d\theta}{ds} \tag{3.11}$$

where s is the proper distance and θ denotes the angular coordinate along the geodesic motion on S^3. We treat geodesics which are related by a translation in t and on S^3 as equivalent. The geodesic satisfies the equation

$$\frac{1}{f}\left(\frac{dr}{ds}\right)^2 + \frac{q^2}{r^2} - \frac{1}{f}E^2 = 1 \ . \tag{3.12}$$

Equation (3.12) is precisely (3.7) with the identification[10]

$$f\mathcal{Z}' = \frac{dr}{ds}, \qquad u = iE, \qquad k = iq \ . \tag{3.13}$$

κ_r of (3.5) can be identified as the proper velocity of the geodesic along the r direction. Thus $Z(u,k)$ can be associated with a (complex) spacelike geodesic with constants of

[10]The sign choice for the first expression below corresponds to having the geodesic moving away from the boundary, while those for the last two equations are for convenience. The fact i in relating the boundary "velocities" u, k to the velocities E, q of the bulk geodesic is due to that the geodesic is spacelike.

motion $E = -iu$ and $q = -ik$, which starts and ends at $r = +\infty$.[11] More explicitly, one finds that $Z(u,k)$ can be written as

$$Z(u,k) = -Et(E,q) - L(E,q) + qd(E,q) \tag{3.14}$$

where $L(E,q)$ is the (regularized) proper distance of the geodesic, $t(E,q)$ is the time separation and $d(E,q)$ is the proper distance on S^3 between the final and initial points,

$$\begin{aligned} L(E,q) &= 2\lim_{r\to\infty}\left(\int_{r_c}^{r}\frac{dr}{\sqrt{f+E^2-\frac{f}{r^2}q^2}} - \log r\right) \\ t(E,q) &= 2E\int_{r_c}^{\infty}\frac{dr}{f\sqrt{f+E^2-\frac{f}{r^2}q^2}} \\ d(E,q) &= 2q\int_{r_c}^{\infty}\frac{dr}{r^2\sqrt{f+E^2-\frac{f}{r^2}q^2}}\ . \end{aligned} \tag{3.15}$$

Also note the relation

$$\frac{\partial Z}{\partial E} = -t(E,q) \qquad \frac{\partial Z}{\partial q} = d(E,q) \tag{3.16}$$

which shows that $L(t,d)$ and $Z(E,q)$ are related by a Legendre transform.

Note that E and q do not specify a geodesic uniquely. (3.15) defines a complex geodesic with a choice of root $r_c(E,q)$ of equation (3.6) as the turning point and a contour from $r_c(E,q)$ to $+\infty$. For the same value of E,q, a different choice of the root or a different contour which cannot be smoothly deformed into the previous one defines a different complex geodesic. The identification (3.14) with the boundary $Z(u,k)$ selects a specific one among them.

In the above discussions we have concentrated on the Wightman functions.[12] A similar relation with bulk geodesics can be established for retarded and Feynmann functions in momentum space, whose story is more complicated since their dependence on ν is not uniform. Special care is needed when ν is an integer.[13] This makes the large ν limit more subtle. Even at the leading order, one has to take into account of an infinite number of classical paths in the WKB approximation [37]. Fortunately, all these additional complications arise due to the asymptotic behavior of $f \sim r^2$ near the boundary of spacetime and do not seem to give additional insight into the question of physics beyond the horizon.

3.3 Coordinate space correlation functions

We now look at the Fourier transform of $G_+(\omega,l)$ to the coordinate space correlator (see the appendix for notations)

$$G_+(t;e,e') = \frac{1}{4\pi^2}\sum_{l=0}^{\infty}2(l+1)C_l(e\cdot e')\int_{-\infty}^{\infty}\frac{d\omega}{2\pi}\,e^{-i\omega t}\,G_+(\omega,l)\ . \tag{3.17}$$

[11] Note that depending on the values of E and q the starting and end points can be on the same or different boundaries.

[12] Wightman functions already contain all the information of the theory. For example, Feynmann and retarded functions can be obtained from them.

[13] This can be seen also from zero temperature correlation functions.

The two-sided correlator (2.14) can be obtained from (3.17) by taking $t \to t - i\frac{\beta}{2}$, while the Euclidean correlator $G_E(\tau; e, e')$ can be obtained by taking $t = -i\tau$ with $0 < \tau < \beta$.

In the large ν limit (3.1), using (3.9) we can approximate the sum over l in (3.17) by an integral over k

$$G_+(t,\theta) \approx \frac{\nu^3}{8\pi^3 i \sin\theta} \int_{-\infty}^{\infty} du dk\, k\, e^{-i\nu ut + i\nu k\theta}\, 2\nu e^{\nu Z(u,k)} \tag{3.18}$$

where $\theta = \cos^{-1}(e \cdot e')$ and we have extended the integration range for k to $(-\infty, \infty)$ using that Z is an even function of k. (3.18) can be evaluated by the method of steepest descent with the saddle points determined by

$$\frac{\partial Z}{\partial u} = it, \qquad \frac{\partial Z}{\partial k} = -i\theta \ . \tag{3.19}$$

Using equations (3.16) and (3.13) we find that (3.19) become

$$t = t(E,q), \qquad \theta = d(E,q) \tag{3.20}$$

i.e. bulk geodesics with end point separation given by (t, θ) appear as saddle points of (3.18). Since from (3.14) the regularized geodesic distance $L(t,\theta)$ and $Z(u,k)$ are related by a Legendre transformation, one finds that

$$G_+(t,\theta) \approx \sum_i 2\nu J_i^{\frac{1}{2}} \left(\frac{\nu}{2\pi}\right)^2 e^{-\nu L_i} \left(1 + O(\nu^{-1})\right) \tag{3.21}$$

where i sums over the saddles along the steepest descent contour. The Jacobian J is due to the Gaussian integration around the saddle points.

Some remarks:

1. J can be interpreted as the density of the geodesics. It is proportional to the Van Vleck-Morette determinant for the geodesics. One can check that (3.21) agrees precisely (including the prefactor J) with the expression obtained directly from the geodesic approximation to the coordinate space path integral

$$G(x, r; x', r') = \sum_{paths} e^{\frac{i}{\hbar} mS} \ , \tag{3.22}$$

   after taking the end points to the boundary.

2. In the standard geodesic approximation to (3.22), it is often a subtle question in Lorentzian signature to determine which geodesics contribute to the sum (3.21). In our approach, the steepest descent approximation of the Fourier transform (3.17) gives a *precise* prescription for determining the sum.

3. Higher order terms in (3.21) can be computed systematically in our approach.

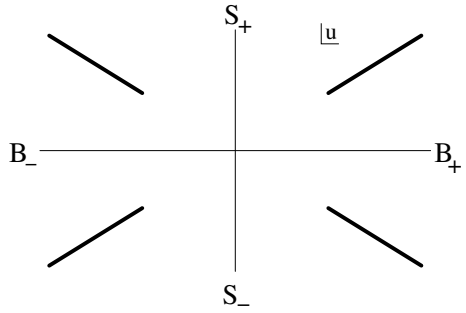

Figure 4: The structure of branch cuts of $Z(u)$ and $r_c(u)$ for $r_0 = 1, r_1 = 2$. At finite ν, the branch cuts become the pole lines of $G_+(\omega, l = 0)$ as in figure 2. The asymptotic regions are labelled by $S_\pm$ or $B_\pm$, indicating whether the turning point for the corresponding u approaches the singularity ($S_\pm$) or the boundary ($B_\pm$).

4. Black hole singularites in Yang-Mills theory

In this section we discuss how information about the black hole singularity can be extracted from $Z(u, k)$ using its relations with the bulk geodesics developed in the last section. For simplicity, we restrict our discussion to $k = 0$, in which case the corresponding bulk geodesic has zero angular momentum. The discussion for general k is more involved and will appear in [23]. The $k = 0$ case already captures many of the essential elements.

4.1 Probing the physics beyond the horizon and near the singularity

We first consider the analytic continuation of $Z(u, k = 0)$[14] to general complex u. We will see that the analytic continuation allows us to probe the regions beyond the horizon and near the singularity.

As discussed in section 2.3, when $u > 0$, the turning point $r_c(u)$ in (3.10) lies outside the horizon, i.e. $r_c > r_0$. The integration contour runs along the positive real r-axis from r_c to $+\infty$. The analytic continuation of $Z(u)$ to the full complex u-plane involves the following two aspects:

1. Analytically continue the turning point $r_c(u)$ from that for real $u > 0$;

2. Smooth deformation of the integration contour as r_c moves on the complex r-plane.

Both steps have some subtleties, which we now discuss in detail.

The analytic continuation of r_c from the $u > 0$ region is not unique, since $r_c(u)$ has branch points in the complex u-plane at which it merges with other solutions of (3.6). These are also branch points of $Z(u)$. When $k = 0$ (3.6) is a quadratic equation for r^2 and $r_c(u)$ coincides with other roots when

$$(u^2 - 1)^2 + 4\mu = 0 \ . \tag{4.1}$$

[14] In the following, we will simply write it as $Z(u)$ and similarly use $G_+(\omega)$ for $G_+(\omega, l = 0)$.

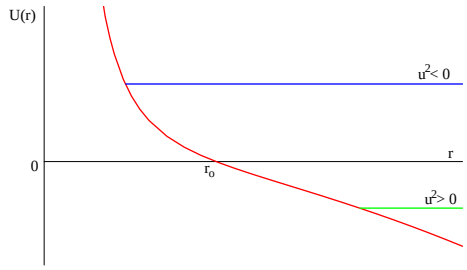

Figure 5: A radial spacelike geodesic can be described by a particle of energy $-u^2$ moving in the potential $U = -f$. The horizon is at $r = r_0$. For $u^2 < 0$, the turning point lies inside the horizon.

From (4.1) we find that $r_c(u)$ has four branch points at

$$u_0 = \pm(r_1 \pm i r_0) = \pm\frac{2\pi}{\overline{\mathcal{B}}}, \pm\frac{2\pi}{\mathcal{B}} \ . \tag{4.2}$$

For r_c and Z to be single-valued on the u-plane, branch cuts have to be specified. Different choices of the branch cuts correspond to different ways of performing the analytic continuation. The locations of the branch cuts cannot be determined from the integrals (3.10) or (3.15) alone. To determine them we need to use analytic properties of $G_+(\omega)$. As discussed around equation (2.23), the only singularities of $G_+(\omega)$ at finite ν are four lines of poles located at

$$u \approx \frac{2\pi}{\overline{\mathcal{B}}} + \frac{\omega_0}{\nu} + \frac{4\pi n}{\nu\overline{\mathcal{B}}}, \qquad n = 0, 1, \cdots \ . \tag{4.3}$$

and the reflections of (4.3) with respect to the real and imaginary u axes. In the large ν limit, since the spacings between poles go to zero, these lines of poles become branch cuts of $Z(u)$.[15] This determines the directions of the branch cuts to be along the radial direction from each branch point to infinity (see figure 4).

With the branch cuts precisely specified, $r_c(u)$ can now be uniquely determined from that for $u > 0$. In particular, figure 4 implies that the analytic continuation should be done through the region around $u = 0$. To to be definite, let us concentrate on real u^2. In this case, a convenient way to visualize how the turning point changes with u is to treat equation (3.12) as the motion of a one-dimensional particle of energy $E^2 = -u^2$, moving in a potential[16]

$$U = -V = -f \ , \tag{4.4}$$

as in figure 5. For real u, $r_c > r_0$, i.e. the turning point lies outside the horizon, while for u pure imaginary, $r_c < r_0$ and the the turning point lies inside the horizon. One can also

[15] The simplest example exhibiting this behavior is a Gamma-function $\Gamma(\nu z)$. The function has poles along the negative real axis for finite ν. In the large ν limit, upon using the Stirling formula, the pole line is replaced by a branch cut.

[16] Note the potential V is inverted since we work in the classically forbidden region of the Schrodinger problem (2.15).

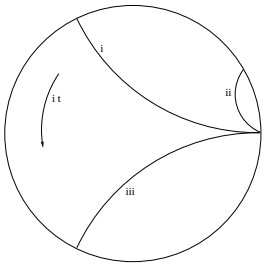

Figure 6: Radial geodesics in the Euclidean section of the spacetime which corresponds to real values of u. The Euclidean section of the $r-t$ plane is a disk with it as the angular coordinate and the origin of the disk at $r = r_0$. The solid circle is the boundary. Geodesics with $u > 0$ (i and ii) and $u < 0$ (iii) are schematically plotted. Geodesic ii correspond to the large u limit, in which case the tuning point is close to the boundary and the end points of the geodesic are nearly coincidental.

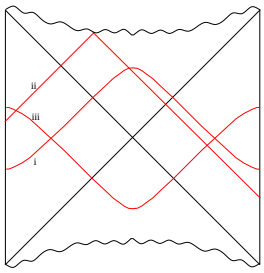

Figure 7: Radial geodesics in the Lorentzian section of the spacetime corresponding to pure imaginary values of $u = iE$ are schematically plotted. Geodesics i and ii have $E > 0$ while iii has $E < 0$. Geodesic ii correspond to the limit $E \to +\infty$, in which case the tuning point is close to the singularity and the geodesic becomes nearly null.

solve (3.6) explicitly and $r_c(u)$ is given by the positive branch of the equation

$$r_c^2 = \sqrt{\mu + \left(\frac{1-u^2}{2}\right)^2} - \frac{1-u^2}{2}\,. \tag{4.5}$$

With the turning point specified, one can now find the bulk geodesics corresponding to various values of u from simple geometric considerations. For example, real values of u correspond to radial geodesics in the Euclidean section of the spacetime (see figure 6), since from (3.13) and (3.11) t is pure imaginary along the geodesics. Pure imaginary values of $u = iE$ (E real) correspond to real geodesics in the Lorentzian section of the spacetime, which connect two asymptotic boundaries (see figure 7). The turning point of such a geodesic lies in region II for $E > 0$ and in region IV for $E < 0$ (see also figure 1).

The dependence of r_c on u illustrates some interesting features in the relation between bulk and boundary scales. For real $u \to \pm\infty$, the turning point is given by

$$r_c \approx |u| \to +\infty \tag{4.6}$$

i.e. the turning point approaches the boundary. In this limit, the end points of the geodesic becomes nearly coincidental. When u decreases, r_c also decreases. The turning point r_c reaches the horizon for $u = 0$. This behavior reflects a familiar feature of the AdS/CFT

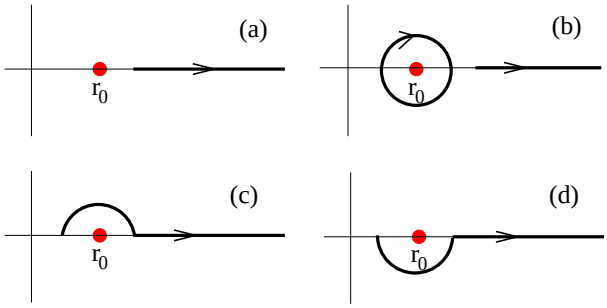

Figure 8: The integration contours in the complex r-plane for (a): $u > 0$, (b): $u < 0$, (c): $u = iE, E > 0$, (d): $u = iE, E < 0$. The solid dot indicates the pole $r = r_0$ of the integrand (horizon).

correspondence, called IR/UV connection [1, 38], which relates long distances in the AdS spacetime to high energies in the boundary theory. The turning point r_c moves inside the horizon when u moves along the imaginary axis from the origin. Let $u = iE$. Then as $|E|$ increases, r_c decreases (see equation (4.5)). For $|E| \to +\infty$, we find that

$$r_c \approx \frac{\sqrt{\mu}}{|E|} \to 0 \tag{4.7}$$

i.e. the turning point approaches the singularity. Thus when dealing with physics inside the horizon, there appears to be a new feature. To probe deeper inside the horizon requires larger E. Since the singularity may heuristically be considered as the UV of the bulk, we find a UV/UV connection. It is important to keep in mind that inside the horizon, r plays the role of the time coordinate. This indicates that the "time" inside the horizon is indeed holographically generated from the boundary Yang-Mills theory.

The above discussions can be easily generalized to all complex values of u using equation (3.6). In particular, from (3.6), $|r_c| \to 0$ requires that $|u| \to \infty$, due to the fact that f blows up at the singularity (large curvature effect). Conversely, $|u| \to \infty$ implies either $|r_c| \to 0$ or $|r_c| \to +\infty$. Thus along different directions to infinity in the complex u-plane, the turning point either approaches the boundary or the singularity. The branch cuts in figure 4 divide the complex infinity of the u-plane into various asymptotic regions. The regions which correspond to the singularity or the boundary are indicated in figure 4. Near the real u axis, the turning point approaches the boundary as $|u| \to +\infty$. As $|u| \to +\infty$ near the imaginary u axis, the turning point approaches the singularity.

We now look at the second aspect of the analytic continuation of $Z(u)$. This involves the deformation of the integration contour in (3.10) (or (3.15)) as $r_c(u)$ moves in the complex r-plane. As the contour is deformed, one needs to be careful about the contribution of the pole at $r = r_0$ of the $1/f$ factor in the integrand. To find the contribution of the pole, it is enough to consider when the turning point is close to the pole.[17] This happens when $|u|$ is small, in which case a prescription for the contour deformation can be obtained

[17] f also has other poles at $-r_0$ and $\pm ir_1$. The analytic continuation procedure is such that the turning point never coincides with these poles.

from the requirement that $Z(u)$ be analytic at $u = 0$. The contours for other values of u can then be obtained by continuous deformation without further subtlety. The resulting contours for real and pure imaginary u's are plotted in figure 8, from which the contribution of the pole can be readily obtained.

For real $u < 0$, the contribution from the pole to $t(u)$ of (3.15) is $-i\beta$. This is precisely the period of the complex time and matches with the geometric picture of figure 6. When $u = iE$ for real E, the imaginary part of $t(u)$ solely comes from the pole contribution and we find

$$\mathrm{Im}\, t(iE) = -\frac{i\beta}{2}, \qquad E \ \text{real}\,. \tag{4.8}$$

This shows that the end point of the corresponding geodesic lies in the other asymptotic boundary, i.e. region III of figure 1, again consistent with figure 7.

To summarize, through the function $r_c(u)$, we establish a correspondence between the complex u- and r-planes. $G_+(\nu u)$ evaluated at u in the large ν limit probes the black hole geometry near $r_c(u)$. The boundary correlation functions encode not only the bulk geometry outside the horizon, but also regions beyond the horizon and near the singularity.

We emphasize that the proper identification of the branch cuts for $Z(u)$ and $r_c(u)$ (which in turn depends on the knowledge of poles for $G_+(\omega)$) is crucial for our conclusion above. Different choices of the branch cuts could lead to completely different physical pictures. For example, a different analytic continuation procedure may lead to a $r_c(iE)$ that for real E is not given by the positive branch of (4.5), but some other root of the turning point equation (3.6). In that case one cannot associate the geodesics in figure 7 with $G_+(\omega)$ and it is not clear one could probe the physics beyond the horizon.

Given $Z(u)$ from the large ν limit of the boundary $G_+(\nu u)$, the problem of finding the bulk metric is essentially a classical inverse scattering problem. Due to the large number of isometries of the background, the problem is effectively one-dimensional, being that of a particle moving in (4.4). The equivalent one-dimensional problem can be phrased as follows. Consider sending a particle toward the potential from $r = \infty$ and waiting for it to come back. $L(E)$ is then the (regularized) time interval for this scattering process. With the knowledge of $L(E)$ for all values of E, one can in principle reconstruct the potential (4.4). At a given E, $L(E)$ probes the behavior of the potential (4.4) near the turning point $r_c(u)$.

4.2 Manifestations of singularities in boundary theories

We have found that the geometry around the black hole singularity is encoded in the behavior of $G_+(\omega)$ near the imaginary infinity. We now examine the manifestations of the singularity explicitly.

The integrals in (3.15) can be evaluated explicitly and one finds[18]

$$\begin{aligned} L(u) &= -\frac{1}{2}\log(A_+\widetilde{A}_+A_-\widetilde{A}_-) + 2\log\frac{|B|}{2\pi} \\ t(u) &= \frac{\beta}{4\pi}\log\left(\frac{A_+\widetilde{A}_-}{A_-\widetilde{A}_+}\right) - i\frac{\widetilde{\beta}}{4\pi}\log\left(\frac{A_+\widetilde{A}_+}{A_-\widetilde{A}_-}\right) - \frac{i\beta}{2} \end{aligned} \tag{4.9}$$

[18]The expressions below were obtained before in [12] in a somewhat different form.

and

$$A_\pm = \frac{1}{2} \pm u\frac{\mathcal{B}}{4\pi}, \qquad \widetilde{A}_\pm = \frac{1}{2} \pm u\frac{\overline{\mathcal{B}}}{4\pi} \tag{4.10}$$

In (4.9) the branch cuts of the logarithms are chosen to be straight lines extending radially from $\pm\frac{2\pi}{\mathcal{B}}$ and $\pm\frac{2\pi}{\overline{\mathcal{B}}}$ to ∞, as follows from the discussion in previous subsection (see figure 4).

Expanding (4.9) for large $|u|$ we find that $L(u)$ and $t(u)$ of (3.15) can be written as

$$\begin{aligned} L(u) &= -2\log\left(\frac{[u]}{2}\right) + \sum_{n=1}^{\infty} \frac{a_{2n}}{2n}\frac{1}{u^{2n}} \\ t(u) &= t_0 - i\frac{2}{u} - i\sum_{n=1}^{\infty} \frac{a_{2n}}{2n+1}\frac{1}{u^{2n+1}} \end{aligned} \tag{4.11}$$

which lead to the expansion for $Z(u)$

$$Z(u) = iut_0 + 2\log\tfrac{[u]}{2} + 2 - \textstyle\sum_{n=1}^{\infty} \frac{a_{2n}}{2n(2n+1)}\frac{1}{u^{2n}} \ . \tag{4.12}$$

In (4.11) and (4.12),

$$a_n = \left(\frac{2\pi}{\mathcal{B}}\right)^n + \left(\frac{2\pi}{\overline{\mathcal{B}}}\right)^n$$

and t_0 and $[u]$ are given by

$$t_0 = \begin{cases} 0 & u \in B_+ \\ -i\beta & u \in B_- \\ \frac{\overline{\mathcal{B}}}{2} & u \in S_+ \\ -\frac{\mathcal{B}}{2} & u \in S_- \end{cases}, \qquad [u] = \begin{cases} u & u \in B_+ \\ -u & u \in B_- \\ -iu & u \in S_+ \\ iu & u \in S_- \end{cases}, \tag{4.13}$$

where $B_\pm$ and $S_\pm$ denote asymptotic regions in figure 4 whose corresponding turning point approaches the boundary and the singularity respectively. The values of t_0 for various limits can be easily understood from the geometric pictures of the geodesics in figures 6 and 7. When $u \to \pm\infty$, the end points of the Euclidean geodesics become nearly coincidental. The value $-i\beta$ for $u \to -\infty$ is precisely the full period of the Euclidean circle. When $u \to \pm i\infty$, the bouncing geodesics in figure 7 become nearly null and the corresponding values of t_0 in (4.13) are twice of those in (2.5).

Equations (4.12) implies that as $\omega = \nu u \to \pm i\infty$, the boundary correlation function behaves as

$$G_+(\omega, l=0) \approx \frac{1}{\pi(\Gamma(\nu))^2}\left(\mp i\frac{\omega}{2}\right)^{2\nu} e^{i\omega\left(\pm\frac{\widetilde{\beta}}{2} - \frac{i\beta}{2}\right)}\left(1 + O\left(\frac{1}{\omega^2}\right)\right) \tag{4.14}$$

where the upper (lower) sign corresponds to $\omega \to +i\infty$ ($-i\infty$). Note that the correlation function decays exponentially along these directions. For $\omega \to \pm\infty$ near the real axis, we find

$$G_+(\omega, l=0) \approx \begin{cases} \frac{1}{\pi(\Gamma(\nu))^2}\left(\frac{\omega}{2}\right)^{2\nu}\left(1 + O\left(\frac{1}{\omega^2}\right)\right) & \omega \to +\infty \\ \frac{1}{\pi(\Gamma(\nu))^2}\left(-\frac{\omega}{2}\right)^{2\nu} e^{\beta\omega}\left(1 + O\left(\frac{1}{\omega^2}\right)\right) & \omega \to -\infty \end{cases} . \tag{4.15}$$

While equations (4.14) and (4.15) were derived in the large ν limit, they should hold for finite ν, since the $|u| \to \infty$ limit should coincide with the limit $|\omega| = \nu|u| \to \infty$ regardless

of the value of ν. Note that (4.15) is precisely what one would expect of the large frequency behavior of a conformal field theory at finite temperature.[19] The exponential falloff in (4.14) reflects the presence of a curvature singularity in the bulk. The falloff is controlled by the complex parameter $\mathcal{B}$ (introduced in (2.6)) which characterizes the black hole geometry.

4.3 Generalizations to nonzero angular momentum

The above discussions can be extended to Wightman functions of nonzero angular momenta. We summarize some main results here, leaving detailed discussions to [23]:

1. For boundary angular velocity k real, which corresponds to geodesics of pure imaginary angular momentum, the structure of the branch cuts for $Z(u,k)$ is similar to figure 4. The locations of the branch points and the directions of the branch cuts depend nontrivially on k. At finite ν, the branch cuts become lines of poles of $G_+(\omega,l)$.

2. For bulk geodesics with real angular momentum q, an important new feature appears: there exist geodesic orbits with constant real r. The existence of such orbits leads to the appearance of virtual states (if there is an orbit lying inside the horizon) or bound states (if there is an orbit lying outside the horizon) in the Schrodinger problem (2.15). These virtual states or bound states lead to two new lines of poles of $G_+(\omega,l)$ along the imaginary ω-axis for pure imaginary l. Thus $Z(u,k)$ has two new branch cuts along the imaginary u-axis for $k=iq$ pure imaginary.

3. It remains true that the turning point approaches the boundary (singularity) for $|u|\to\infty$ along the real (imaginary) axis. Furthermore, for any fixed l, in the large ω limit, equations (4.14)–(4.15) remain valid.

4. In the limit that q goes to zero, the branch cuts for $Z(u,iq)$ along the imaginary axis move to infinity and figure 4 is recovered. The fact that there are branch points at $u=\pm i\infty$ at $q=0$ leads to interesting behaviors in the expansion of $Z(u,k)$ around $k=0$. For example, let $u=iE$ with real E, then one finds that to leading order in the limit $E\to+\infty$, $Z(u,k)$ has the following small k expansion[20]

$$Z(iE,k)\approx -E\frac{\overline{\mathcal{B}}}{2}+2\log\frac{E}{2}+2+\frac{1}{E^2}\sum_{l=1}^{\infty}a_l\left(k^2E^2\right)^l+\cdots \tag{4.16}$$

with

$$a_1=-\frac{\pi}{2\mu^{\frac{1}{2}}},\qquad a_2=\frac{3\pi}{16\mu^{\frac{3}{2}}},\qquad a_l\sim\frac{1}{\mu^{\frac{2l-1}{2}}} \tag{4.17}$$

where μ dependence can be deduced based on dimensional analysis. Note that the expansion parameter for small k is given by k^2E^2 and the derivatives over k at $k=0$ become divergent in the large E limit. We will see in the next section that (4.16) leads to divergences in certain gauge invariant observables in the boundary theory.

[19] When real $\omega\to+\infty$, one expects the correlation function to recover the zero temperature result. The second line of equation (4.15) follows from the general properties of the Wightman function at finite temperature.

[20] Note that the equation below is obtained by first doing a small k expansion and then taking leading order terms in $1/E$.

We also mention by passing a few other generalizations:

5. The discussions of this section can also be generalized to an AdS_{d+1} black hole of dimension $d \geq 2$ [23]. All the essential features for AdS_5 black holes carry over to other dimension $d \geq 3$. A special case is a BTZ black hole in AdS_3, which has an orbifold singularity and the story is somewhat different. In the BTZ case, the corresponding Schrodinger equation (2.15) can be exactly solved and the relation between the large ν limit of Wightman functions and bulk geodesics can be explicitly verified.

6. The subdominant contributions in (3.9) can also be worked out using a more sophisticated WKB method involving more than one turning point. One can show that an infinite number of subdominant contributions become important at the branch cuts[21] where they add up to produce the poles of $G_+(\omega, l)$. In [24] we use this property to derive the positions of poles of G_+ for general l and dimension in the large ν limit.

7. While we have not examined it in detail, it is interesting to compute the higher order $1/\nu$ corrections in (3.9). In particular, the function $Q(z)$ (3.2) will start contributing at the order $O(1/\nu)$. Since $Q(z)$ becomes singular at $r \to 0$, it would be interesting to see whether it yields new manifestations of the singularity in the boundary theory correlation functions.

4.4 Coordinate space correlators and alternative indications of curvature singularities

In this subsection we consider the Fourier transform of $G_+(\omega, l)$ to coordinate space. To make connection to the result of [12], we consider

$$G_{12}(t, \theta = 0) = G_+\left(t - \frac{i\beta}{2}, \theta = 0\right) \tag{4.18}$$

which can be obtained from (3.17) by taking $t \to t - \frac{i\beta}{2}$ and corresponds to inserting operators on two different boundaries. We restrict to $\theta = 0$ for simplicity. In the large ν limit, G_{12} can be evaluated in exact parallel of the discussion of section 3.3. One can approximate the sum over l by an integral

$$G_{12}(t) \approx \frac{\nu^4}{8\pi^3} \int_{-\infty}^{\infty} du dk\, k^2\, e^{-i\nu u t - \frac{1}{2}\nu u \beta}\, 2\nu e^{\nu Z(u,k)} \tag{4.19}$$

and perform the integrals using the saddle point method.

From the discussion of section 3.3, the saddles of (4.19) correspond to geodesics whose end points lie on different boundaries and are separated in time by an amount t and no

[21] In other words, the branch cuts are anti-Stokes lines for an infinite number of subdominant exponentials. The Stokes lines can be obtained from the branch cuts by rotating $\pm\frac{\pi}{2}$. A simple example which also exhibits this phenomenon is the Gamma-function (see e.g. [39]).

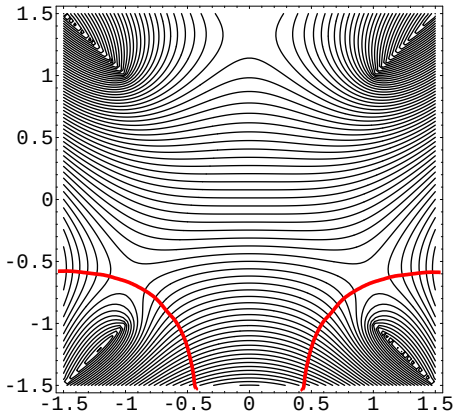

Figure 9: The contour plot for the real part of $Z(u, k = 0) - iu(t - i\frac{\beta}{2})$ for $t < \frac{\widetilde{\beta}}{2}$ in the complex u-plane. There is a saddle on the imaginary axis and two complex ones. The steepest descent contour is also shown in figure. The contour does not pass through the saddle on the imaginary axis even if it dominates.

separation on S^3. The saddle for the k-integral is simply $k = 0$. The saddles for the u-integral are given by

$$\frac{\partial Z(u, k = 0)}{\partial u} = it + \frac{\beta}{2} \, . \tag{4.20}$$

Note that $Z(u, k = 0)$ can be obtained from (4.9). The solutions to (4.20) can be visualized conveniently on the contour plot of the real part of $Z(u, k = 0) - iu(t - i\frac{\beta}{2})$ in the complex u-plane. See figure 8. In the figure we also indicate the steepest descent paths to which the integration contour of (4.19) can be deformed.

The dependence of the saddle point structure on t can be summarized as follows. For $t < t_c = \frac{\widetilde{\beta}}{2}$, there are three saddles, as indicated in figure 8. The one on the imaginary axis corresponds to a real geodesic in Lorentzian black hole spacetime with a turning point inside the horizon (see figure 7). This is the bouncing geodesic discussed by [12]. We will refer to this saddle as the bouncing saddle below. The other two saddles describe complex geodesics, which do not seem to probe the physics beyond the horizon. As t approaches t_c, the bouncing saddle moves to infinity along the imaginary axis and the turning point of the geodesic approaches the singularity. For $t > t_c$, the bouncing saddle disappears.[22]

From the steepest descent contour, we conclude that the bouncing geodesic does not contribute to coordinate space correlation functions. This result was obtained in [12] by analytical continuation from Euclidean signature.[23] Here we confirm their result.

[22] For $t > t_c$, the two complex saddles wind around the branch points at $\frac{2\pi}{\mathcal{B}}$ and $-\frac{2\pi}{\mathcal{B}}$ respectively and approach them as $t \to \infty$.

[23] In [12] it was argued that the information regarding the bouncing geodesics and thus the singularity can nevertheless be obtained by analytic continuation in the large ν limit, since there exist certain values of t for which the bouncing saddle merges with other saddles.

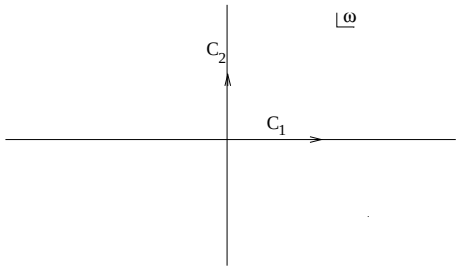

Figure 10: The integration contours for $G_{12}(t)$ ($\mathcal{C}_1$) and $H_{12}(\tau)$ ($\mathcal{C}_2$).

4.5 New observables of the boundary theory and manifestations of the curvature singularity

While the bouncing geodesic does not contribute to (4.18) directly, from momentum space correlation functions, we can easily construct observables in the boundary theory which are approximated by the bouncing geodesics in the large ν limit.

Let us start with two-sided correlator (4.18) with coincidental spatial coordinates

$$\begin{aligned} G_{12}(t) &= \mathrm{Tr}\left[e^{-\beta H}\mathcal{O}(t-i\beta/2,e)\mathcal{O}(0,e)\right] \\ &= \frac{1}{4\pi^2}\sum_{l=0}^{\infty} 2(l+1)^2 \int_{\mathcal{C}_1}\frac{d\omega}{2\pi}\, e^{-i\omega t} G_{12}(\omega,l) \end{aligned} \tag{4.21}$$

where the contour $\mathcal{C}_1$ is along the real ω-axis and

$$G_{12}(\omega,l) = e^{-\frac{\omega\beta}{2}} G_+(\omega,l)\,. \tag{4.22}$$

From (4.14)–(4.15) and the comments in section 4.3 regarding their generalizations to nonzero l, we find that the large ω behaviors of $G_{12}(\omega,l)$ are given by

$$G_{12}(\omega,l) \approx \begin{cases} \frac{1}{\pi(\Gamma(\nu))^2}\left(\mp i\frac{\omega}{2}\right)^{2\nu} e^{\pm\frac{i\omega\widetilde{\beta}}{2}} & \omega\to\pm i\infty \\ \frac{1}{\pi(\Gamma(\nu))^2}\left(\pm\frac{\omega}{2}\right)^{2\nu} e^{\mp\frac{\beta\omega}{2}} & \omega\to\pm\infty \quad \mathrm{cr} \end{cases} \tag{4.23}$$

We now construct new observables in the boundary theory

$$H_{12}(\tau) = \frac{1}{4\pi^2}\sum_{l=0}^{\infty} 2(l+1)^2 \int_{\mathcal{C}_2}\frac{d\omega}{2\pi}\, e^{-i\omega\tau} G_{12}(\omega,l) \tag{4.24}$$

where the contour $\mathcal{C}_2$ are along the imaginary axis. $H_{12}(\tau)$ can be defined for $-\frac{\widetilde{\beta}}{2} < \tau < \frac{\widetilde{\beta}}{2}$ due to the exponential falloff (4.23) of $G_{12}(\omega)$ along the imaginary axis. Note that $H_{12}(\tau)$ is gauge invariant by definition. While its existence depends on the asymptotic behavior of $G_{12}(\omega,l)$ along the imaginary ω-axis, it is an object which can in principle be intrinsically defined in the boundary theory.[24]

[24] One can of course define $H_{12}(\tau;e,e')$ for non-coincidental points on S^3. We do not expect divergences for them. They will be discussed in [23].

In the large ν limit (4.24) can be evaluated in exact parallel as (4.18)–(4.19) by approximating the sum over l by an integral and performing the saddle point approximation in the resulting integrals. The only difference is that the integration contour for ω is now along the imaginary axis rather than the real axis. Thus instead of picking up the two complex saddles in figure 8, (4.24) is given by expanding around the bouncing saddle on the imaginary axis.

As $\delta t = t_c - \tau \to 0$, the bouncing saddle moves to the imaginary infinity and the turning point r_c of the corresponding geodesic approaches the singularity. In this limit, we can use (4.16) to approximate $Z(u,k)$. Then the integrals for H_{12} can be written as $(u = iE)$

$$\begin{aligned} H_{12}(\tau) &\sim \int dE \int dk k^2 \ \exp\left[-\nu E\delta t + 2\nu \log\frac{E}{2} + \frac{\nu}{E^2}\sum_{l=1}^{\infty} a_l \left(k^2E^2\right)^l\right] \\ &\sim (E_c)^{2\nu+1}\left(1+\sum_{n=1}^{\infty} c_n \left(\frac{E_c^2}{\nu\sqrt{\mu}}\right)^n\right) \\ &\sim \frac{1}{(\delta t)^{2\nu+1}}\left(1+\sum_{n=1}^{\infty}\frac{b_n}{(\nu\sqrt{\mu}\delta t^2)^n}\right) \end{aligned} \tag{4.25}$$

where the saddle for the k-integral is $k = 0$ and for the E integral is

$$E_c \approx \frac{2}{\delta t} \to \infty \ . \tag{4.26}$$

Note that in (4.25) we have only worked out the qualitative δt dependence in the small δt limit rather than attempting a precise evaluation. The order of limits should be first $\nu \to \infty$ and then $\delta t \to 0$. In evaluating the high order $1/\nu$ terms in (4.25), there are two other sources of $1/\nu$ corrections that we did not take into account: $1/\nu$ corrections in (3.9) and those in turning the sum over l in (4.24) to an integral. Since we are only interested in power counting, apart from magic cancellations, this will not affect the qualitative behaviors in (4.25). The divergences in $1/\nu^n$ terms arise from the k-integral and are due to the structure of the small k expansion in (4.16).

Note that (4.25) is precisely what one expects of a bouncing geodesic as its turning point approaches the singularity. From the bulk point of view, one expects the contribution from the geodesic should take the form[25]

$$J^{\frac{1}{2}} e^{-\nu L}\left(1+\sum_{n=1}^{\infty}\frac{R_n}{\nu^n}\right) \tag{4.27}$$

where L is the regularized the geodesic distance, J is the Van Vleck-Morette determinant. Higher order terms in (4.27) arise from cubic and higher order terms in the sum over paths around the geodesic and R_n can be expressed in terms of bulk geometric quantities in the form of components of curvature tensors (and their derivatives) integrated along the geodesic. In general the explicit expressions for R_n are very complicated (see e.g. [40]). On

[25]Similar argument was also used in [12].

dimensional ground, one expects that in the limit that the turning point approaches the singularity $R_n \sim \frac{1}{\epsilon^n}$, with ϵ the proper time between the turning point and the singularity. This leads to

$$H_{12} \sim J^{\frac{1}{2}} e^{-\nu L} \left(1 + \sum_{n=1}^{\infty} \frac{b_n}{(\nu\epsilon)^n}\right) . \tag{4.28}$$

Equation (4.28) precisely agrees with (4.25) since from the metric (2.2)

$$\epsilon \sim \int_0^{r_c} \frac{dr}{\sqrt{f}} \sim \frac{r_c^2}{\sqrt{\mu}} \sim \frac{\sqrt{\mu}}{E_c^2} \sim \sqrt{\mu}\delta t^2$$

where we have used (4.7) and (4.26).

To summarize we have constructed new gauge invariant observables (4.24) in the boundary theory that are sensitive to the physics beyond the horizon and in particular their behaviors near $\tau \to \frac{\widetilde{\beta}}{2}$ precisely reflect the curvature divergence of the singularity. These observables are related nonlocally in time with (4.18). It would be interesting to better understand their meaning in Yang-Mills theories.[26]

5. Discussions: resolution of black hole singularities at finite N ?

In this paper we established a direct relation between space-like geodesics in the bulk and the large operator dimension limit of the boundary Wightman functions $G_+(\omega, l)$ in momentum space. The results present an intriguing picture on how physics beyond the horizon is encoded in the boundary theory. In particular, it gives a clear indication that the "time" inside the horizon is holographically generated from the thermal Yang-Mills theory.

The poles of $G_+(\omega, l)$ separate the asymptotic region of the complex ω-plane into several sectors (see figures 2 and 4). The sectors near the real axis describe the physics near the boundary while the sectors near the imaginary axis describe the physics near the singularity.[27] We found the following signals of the singularity in the boundary theory:

1. $G_+(\omega, l)$ falls off exponentially for $\omega \to \pm i\infty$ (see equation (4.14) or (4.23)). The falloff is controlled by the complex parameter $\mathcal{B}$ (2.6), which characterizes the black hole geometry.

2. We constructed new observables $H_{12}(\tau)$ (equation (4.24)) in the boundary theory which are related nonlocally in time with coordinate space Wightman functions. The curvature divergence of the singularity is reflected in the divergences of $H_{12}(\tau)$ as $\tau \to \pm\frac{\widetilde{\beta}}{2}$. While the leading order divergence of $H_{12}(\tau)$ (i.e. the prefactor in (4.25))

[26] It seems possible to define a new theory whose momentum space correlation functions evaluated at ω are given by $G_+(i\omega)$. $H_{12}(\tau)$ would correspond to "Euclidean" Green functions in this new theory.

[27] We note that this conclusion does not depend sensitively on whether the curvature singularity lies in the Lorentzian section of spacetime. For example, if one regularizes f in (2.2) by $f = r^2 + 1 - \frac{\mu}{r^2+\epsilon^2}$ with a small ϵ to move to the singularity to the complex r-plane [15], the picture would remain exactly the same, provided this does not change the pattern of quasinormal poles significantly, which should be the case for ϵ small.

can be attributed to 1. above, the divergences in higher order $1/\nu$ terms are due to more delicate behavior of $Z(u,k)$ for small k and $u \to \pm i\infty$.

While the above results were derived in the large ν expansion, the essential features should persist for finite ν. For example, we expect equations (4.14) and (4.16) should be valid for finite ν as well.[28]

We now comment on the implications of our results in resolving the black hole singularity.

The rich analytic behavior observed for G_+ in the complex ω-plane is tied to the fact that in the large N limit, the boundary theory has a continuous spectrum, even though it lives on a compact space. In the bulk, the continuous spectrum arises because of the presence of the horizon. In Yang-Mills theory, the continuous spectrum should be related to the fact that in the high temperature phase, typical states in the thermal ensemble have energy of order N^2.[29]

At finite N, no matter how large, the boundary theory on S^3 has a discrete spectrum. In particular, the finite temperature Wightman function should have the form

$$G_+(\omega) = 2\pi \sum_{m,n} e^{-\beta E_m} \rho_{mn} \delta(\omega - E_n + E_m) \tag{5.1}$$

which is a sum of delta functions along the real ω-axis, where m, n sum over the physical states of the theory. $G_+(\omega)$ in equation (5.1) does not have an unambiguous continuation off the real axis. In particular, the procedures of analytically continuing G_+ to complex ω and taking the large N limit do not commute. Equation (4.14) arises by taking the large N limit first and then doing the analytic continuation. This appears to imply that at finite N, geometric notions associated with a black hole, such as the event horizon and the singularity, no longer exist. This is not surprising since the black hole geometry arises as a saddle point in the path integral of the boundary theory in a $1/N$ expansion. If one does not use such an expansion, the geometric notions lose their meaning. Thus the singularity appears to be resolved at finite N.

The above arguments, however, do not tell us how the singularity is resolved. There are several possibilities according to which the singularity can be resolved in AdS/CFT:

I. The singularity is already resolved by α'-effects in perturbative string theory, i.e. at finite 't Hooft coupling and infinite N.

IIa. The singularity is resolved *only* at finite N. But at infinite N there is a large N phase transition at certain value of the 't Hooft coupling.

IIb. The singularity is resolved *only* at finite N and there is no large N phase transition for any 't Hooft coupling.

[28] This can be checked explicitly using other approximations.

[29] These states have degeneracies of order e^{cN^2} for some constant c in free theory. When turning on interactions, one expects the degeneracy is lifted and the energy levels have spacings of order e^{-cN^2}. This gives rise to a continuous spectrum in the infinite N limit. We thank O. Aharony, M. Douglas and S. Minwalla for a discussion of this point. Also note that in the low temperature phase, the Yang-Mills theory has a discrete spectrum even at $N = \infty$.

JHEP04(2006)044

To see which possibility is realized, it is important to investigate whether the signals of the singularity found this paper and in [12] persist to weak coupling in the large N limit. If the answer is yes, it would strongly suggest possibility IIb above. This would be a very desirable situation since one would then be able to study the black hole singularity in string theory using *weakly* coupled Yang-Mills theory and focusing on the large N limit. If the answer is no, then both I and IIa are possible. In the event that IIa is realized, one should still be able to detect signals of the singularity at weak coupling, even though the precise signals may not be directly obtainable from the results at strong coupling.

In any case, we believe the results in the paper should provide a valuable guide for understanding the black hole singularity in AdS/CFT.

Finally, it would be interesting to apply the techniques we developed in this paper to other backgrounds, like charged or rotating black holes.

Acknowledgments

We would like to thank O. Aharony, M. Douglas, Q. Ejaz, D. Freedman, G. Horowitz, R. Jaffe, M. Kruczenski, S. Mathur, J. Maldacena, S. Minwalla, J. Negele, K. Rajagopal, M. Rozali, A. Scardicchio, R. Schiappa, N. Seiberg, A. Sen, S. Shenker, D. Son, L. Susskind, W. Taylor, B. Wecht and B. Zwiebach for very useful discussions. We also want to thank Center of Mathematical Sciences at Zhejiang university for hospitality during part of the work. This work is supported in part by Alfred P. Sloan Foundation and funds provided by the U.S. Department of Energy (D.O.E) under cooperative research agreement #DF-FC02-94ER40818.

A. Fourier transform on S^3

A complete set of scalar harmonics on S^3 can be written as $Y_{lmm'}(e)$ transforming under $(l/2, l/2)$ representations of $SO(4) = SU(2) \times SU(2)$ with $-l/2 \leq m, m' \leq l/2$. We use e to denote a point on S^3 and $I = (l, m, m')$ to denote the full set of indices. Y_I is normalized so that

$$\int_{S^3} Y^I(e) Y^J(e) = \delta_{IJ}$$
$$\sum_{m,m'} Y_I(e_1) Y_I(e_2) = \frac{1}{4\pi^2} 2(l+1) C_l(e_1 \cdot e_2)$$

with

$$C_l(\cos\theta) = \frac{\sin(l+1)\theta}{\sin\theta}\,.$$

Also note that

$$\nabla^2_{S^3} Y^I = -l(l+2) Y^I$$

where $\nabla^2_{S^3}$ is the Laplace operator on S^3.

Consider a correlation function $G(e, e')$ on S^3 which only depends on the geodesic distance between two points e and e'. It can be expanded as

$$\begin{aligned} G(e, e') &= \frac{1}{4\pi^2} \sum_{l=0}^{\infty} 2(l+1) C_l(e \cdot e') G(l) \\ &= \sum_I G(l)\, Y^I(e) Y^I(e') \,. \end{aligned}$$

References

[1] J.M. Maldacena, *The large-N limit of superconformal field theories and supergravity*, *Adv. Theor. Math. Phys.* **2** (1998) 231 [hep-th/9711200].

[2] E. Witten, *Anti-de Sitter space and holography*, *Adv. Theor. Math. Phys.* **2** (1998) 253 [hep-th/9802150].

[3] S.S. Gubser, I.R. Klebanov and A.M. Polyakov, *Gauge theory correlators from non-critical string theory*, *Phys. Lett.* **B 428** (1998) 105 [hep-th/9802109].

[4] E. Witten, *Anti-de Sitter space, thermal phase transition and confinement in gauge theories*, *Adv. Theor. Math. Phys.* **2** (1998) 505 [hep-th/9803131].

[5] J.M. Maldacena, *Eternal black holes in anti-de-Sitter*, *JHEP* **04** (2003) 021 [hep-th/0106112].

[6] G.T. Horowitz and S.F. Ross, *Possible resolution of black hole singularities from large-N gauge theory*, *JHEP* **04** (1998) 015 [hep-th/9803085].

[7] V. Balasubramanian and S.F. Ross, *Holographic particle detection*, *Phys. Rev.* **D 61** (2000) 044007 [hep-th/9906226].

[8] J. Louko, D. Marolf and S.F. Ross, *On geodesic propagators and black hole holography*, *Phys. Rev.* **D 62** (2000) 044041 [hep-th/0002111].

[9] P. Kraus, H. Ooguri and S. Shenker, *Inside the horizon with AdS/CFT*, *Phys. Rev.* **D 67** (2003) 124022 [hep-th/0212277].

[10] T.S. Levi and S.F. Ross, *Holography beyond the horizon and cosmic censorship*, *Phys. Rev.* **D 68** (2003) 044005 [hep-th/0304150].

[11] S. Hemming, E. Keski-Vakkuri and P. Kraus, *Strings in the extended BTZ spacetime*, *JHEP* **10** (2002) 006 [hep-th/0208003].

[12] L. Fidkowski, V. Hubeny, M. Kleban and S. Shenker, *The black hole singularity in AdS/CFT*, *JHEP* **02** (2004) 014 [hep-th/0306170].

[13] V. Balasubramanian and T.S. Levi, *Beyond the veil: inner horizon instability and holography*, *Phys. Rev.* **D 70** (2004) 106005 [hep-th/0405048].

[14] L. Fidkowski and S. Shenker, *D-brane instability as a large-N phase transition*, hep-th/0406086.

[15] J. Kaplan, *Extracting data from behind horizons with the AdS/CFT correspondence*, hep-th/0402066.

[16] D. Brecher, J. He and M. Rozali, *On charged black holes in anti-de Sitter space*, *JHEP* **04** (2005) 004 [hep-th/0410214].

JHEP04(2006)044

[17] A. Hamilton, D. Kabat, G. Lifschytz and D.A. Lowe, *Local bulk operators in AdS/CFT: a boundary view of horizons and locality*, hep-th/0506118.

[18] U.H. Danielsson, E. Keski-Vakkuri and M. Kruczenski, *Black hole formation in AdS and thermalization on the boundary*, *JHEP* **02** (2000) 039 [hep-th/9912209].

[19] U.H. Danielsson, E. Keski-Vakkuri and M. Kruczenski, *Spherically collapsing matter in AdS, holography and shellons*, *Nucl. Phys.* **B 563** (1999) 279 [hep-th/9905227].

[20] G.T. Horowitz and J. Maldacena, *The black hole final state*, *JHEP* **02** (2004) 008 [hep-th/0310281].

[21] T. Hertog and G.T. Horowitz, *Holographic description of AdS cosmologies*, *JHEP* **04** (2005) 005 [hep-th/0503071].

[22] T. Hertog and G.T. Horowitz, *Towards a big crunch dual*, *JHEP* **07** (2004) 073 [hep-th/0406134].

[23] G. Festuccia and H. Liu, to appear.

[24] G. Festuccia and H. Liu, to appear.

[25] S.W. Hawking and D.N. Page, *Thermodynamics of black holes in anti-de sitter space*, *Commun. Math. Phys.* **87** (1983) 577.

[26] T. Banks, M.R. Douglas, G.T. Horowitz and E.J. Martinec, *AdS dynamics from conformal field theory*, hep-th/9808016.

[27] I.R. Klebanov and E. Witten, *AdS/CFT correspondence and symmetry breaking*, *Nucl. Phys.* **B 556** (1999) 89 [hep-th/9905104].

[28] V. Balasubramanian, P. Kraus and A.E. Lawrence, *Bulk vs. boundary dynamics in anti-de Sitter spacetime*, *Phys. Rev.* **D 59** (1999) 046003 [hep-th/9805171];
V. Balasubramanian, P. Kraus, A.E. Lawrence and S.P. Trivedi, *Holographic probes of anti-de Sitter space-times*, *Phys. Rev.* **D 59** (1999) 104021 [hep-th/9808017].

[29] D.T. Son and A.O. Starinets, *Minkowski-space correlators in AdS/CFT correspondence: recipe and applications*, *JHEP* **09** (2002) 042 [hep-th/0205051].

[30] C.P. Herzog and D.T. Son, *Schwinger-Keldysh propagators from AdS/CFT correspondence*, *JHEP* **03** (2003) 046 [hep-th/0212072].

[31] D. Marolf, *States and boundary terms: subtleties of lorentzian AdS/CFT*, *JHEP* **05** (2005) 042 [hep-th/0412032].

[32] A. Núñez and A.O. Starinets, *AdS/CFT correspondence, quasinormal modes and thermal correlators in $N = 4$ SYM*, *Phys. Rev.* **D 67** (2003) 124013 [hep-th/0302026].

[33] L. Motl and A. Neitzke, *Asymptotic black hole quasinormal frequencies*, *Adv. Theor. Math. Phys.* **7** (2003) 307 [hep-th/0301173].

[34] V. Cardoso, J. Natario and R. Schiappa, *Asymptotic quasinormal frequencies for black holes in non- asymptotically flat spacetimes*, *J. Math. Phys.* **45** (2004) 4698 [hep-th/0403132].

[35] J. Natario and R. Schiappa, *On the classification of asymptotic quasinormal frequencies for D-dimensional black holes and quantum gravity*, hep-th/0411267.

[36] G. Siopsis, *Large mass expansion of quasi-normal modes in AdS_5*, *Phys. Lett.* **B 590** (2004) 105 [hep-th/0402083].

JHEP04(2006)044

[37] G. Festuccia, H. Liu and A. Scardicchio, unpublished.

[38] L. Susskind and E. Witten, *The holographic bound in anti-de Sitter space*, `hep-th/9805114`.

[39] M.V. Berry, *Infinitely many Stokes smoothings in the gamma function*, *Proc. Roy. Soc. Lond. A* **434** (1991) 465.

[40] J.D. Bekenstein and L. Parker, *Path integral evaluation of Feynman propagator in curved space-time*, *Phys. Rev.* **D 23** (1981) 2850.